

SUPPORTING INFORMATION

Microwave-mediated Synthesis of Lead-Free Cesium Titanium Bromide Double Perovskite: A Sustainable Approach

Emmanuel Reyes-Francis,^{1,2} Carlos Echeverría-Arrondo,² Diego Esparza,³ Tzarara López-Luke,¹

Tatiana Soto-Montero,⁴ Monica Morales-Masis,⁴ Silver-Hamill Turren-Cruz,^{2,5,} Iván Mora-*

Seró,^{2,} and Beatriz Julián-López^{2,*}*

¹ Instituto de Investigación en Metalurgia y Materiales, Universidad Michoacana de San Nicolás de Hidalgo, Edificio U, Ciudad Universitaria, Morelia, Mich, C.P. 58030, Mexico.

² Institute of Advanced Materials (INAM), Universitat Jaume I, Av. Sos Baynat, s/n, 12071, Castelló de la Plana, Spain.

³ Unidad Académica de Ingeniería Eléctrica, Universidad Autónoma de Zacatecas. Jardín Juárez 147, Zacatecas Centro, C.P. 98000, Zacatecas, Mexico.

⁴ MESA+ Institute for Nanotechnology, University of Twente, Enschede, 7500 AE, The Netherlands

⁵ Department of Physical Chemistry, Polish Academy of Sciences, Warsaw 01-224, Poland

Supporting Information file contents:

Figure S1. a) Relative percentages and b) average crystallite size (extracted from Scherrer equation) for the Cs_2TiBr_6 and CsBr phases analyzed at different conditions of MW-reaction temperature and time.

Figure S2. XRD patterns showing the temperature effect over the MW synthesis (30 min). In the patterns, \diamond denotes CsBr peaks, and # represents Cs_2TiBr_6 peaks.

Figure S3. a) Relative percentages and b) average crystallite size (extracted from Scherrer equation) for the Cs_2TiBr_6 and CsBr phases analyzed at different reaction temperatures (time fixed at 30 min).

Figure S4. Comparison of XRD diffractograms for the optimized powders: experimental XRD pattern (in green) and simulated XRD pattern (in dark blue) developed *in silico* using DFT calculations and VASP code for the represented Cs_2TiBr_6 crystal structure.

Figure S5. a) SEM photograph of Cs_2TiBr_6 powder, the scale bar represents 1 μm , b) EDS spectrum of the MW-synthesized Cs_2TiBr_6 powder including the Cs:Ti:Br atomic percentage, which fits well with Cs_2TiBr_6 element proportion.

Figure S6. a) XPS spectra of the Cs_2TiBr_6 powder exhibit a high level of resolution for a) Cs $3d$, b) Ti $2p$, c) Br $3d$, and d) O $1s$ (including deconvolution of the different oxygen species present in the sample).

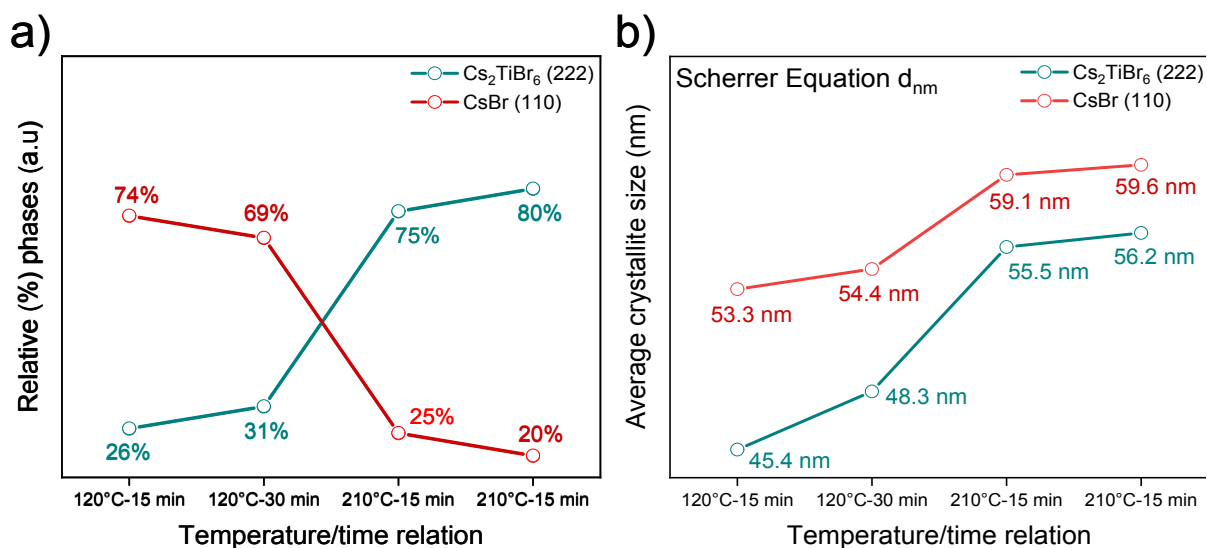


Figure S1. a) Relative mass percentages calculated from XRD patterns (*) and b) average crystallite size (extracted from Scherrer equation) for the Cs_2TiBr_6 and CsBr phases analyzed at different conditions of MW-reaction temperature and time.

(*) X-ray diffraction technique allows quantitative analysis of a crystalline phase (component P) in a solid sample by adding an internal standard s (internal standard method ^[1]). The formula developed by Alexander and Klug is:

$$x_p = kI_p/I_s$$

where k is a coefficient related to the nature of component P and internal standard s , to properties of the X-ray diffraction measurement (i.e., the geometry of the apparatus and the wavelength of the X-ray) and to the amount added from the standard. x_p is the mass % of component P . I_p and I_s are the X-ray diffraction intensities of the more intense hkl peaks of component P and the standard s , respectively.

For the quantitative analysis of our binary mixtures composed of Cs_2TiBr_6 and CsBr , we prepared a set of samples using corundum as standard and CsBr as component P . The experimental XRD patterns provided us with the intensities of the peaks of corundum and CsBr (we considered (104) and (110) planes, respectively) and k was extracted from the equation. Then, we added 10% mass of corundum to our binary mixtures and, with the experimental peak intensities and k , we calculated the mass % of CsBr (x_{CsBr}). The mass % of Cs_2TiBr_6 was directly inferred because $x_{\text{Cs}_2\text{TiBr}_6} + x_{\text{CsBr}} = 1$ (or 100 % in percentage). The representation of the mass % of both phases is given in Figures S1 and S3.

^[1] L. Alexander, H.P. Klug, Basic aspects of X-ray absorption in quantitative diffraction analysis of powder mixtures, *Anal. Chem.*, 20 (1948), 886-889.

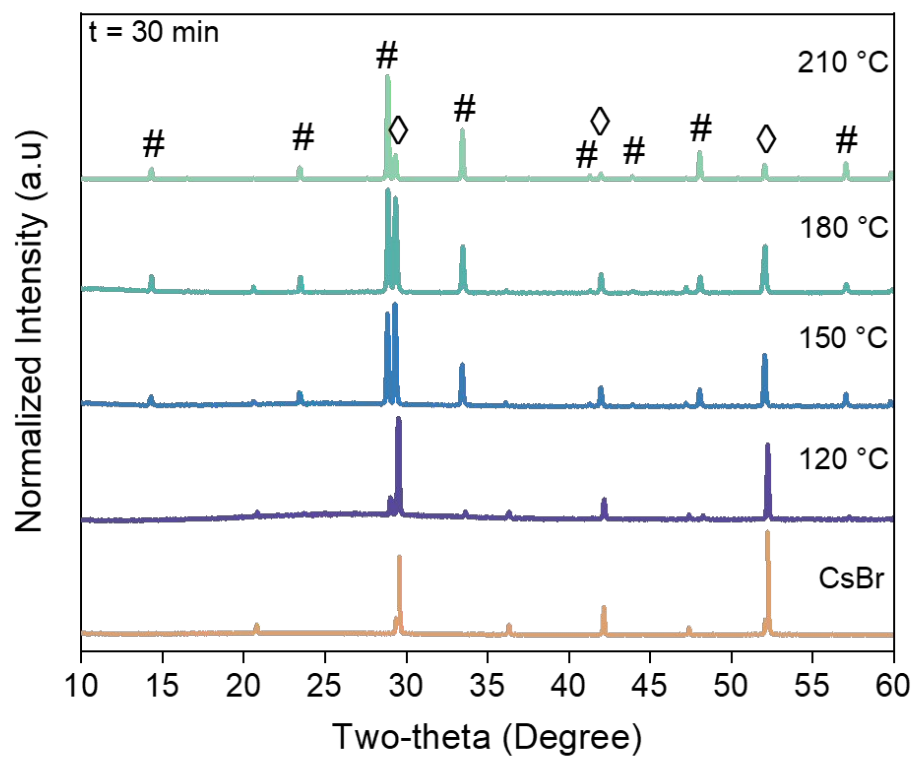


Figure S2. XRD patterns showing the temperature effect over the MW synthesis (30 min). In the patterns, \diamond denotes CsBr peaks, and # represents Cs_2TiBr_6 peaks.

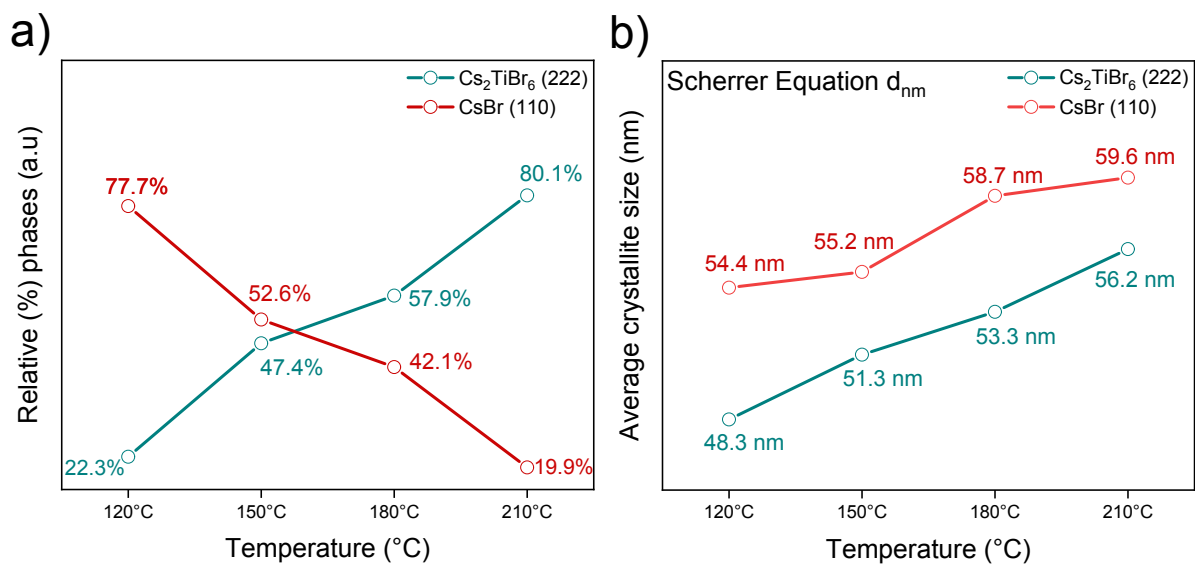


Figure S3. a) Relative mass percentages calculated from XRD patterns and b) average crystallite size (extracted from Scherrer equation) for the Cs_2TiBr_6 and CsBr phases analyzed at different reaction temperatures (time fixed at 30 min).

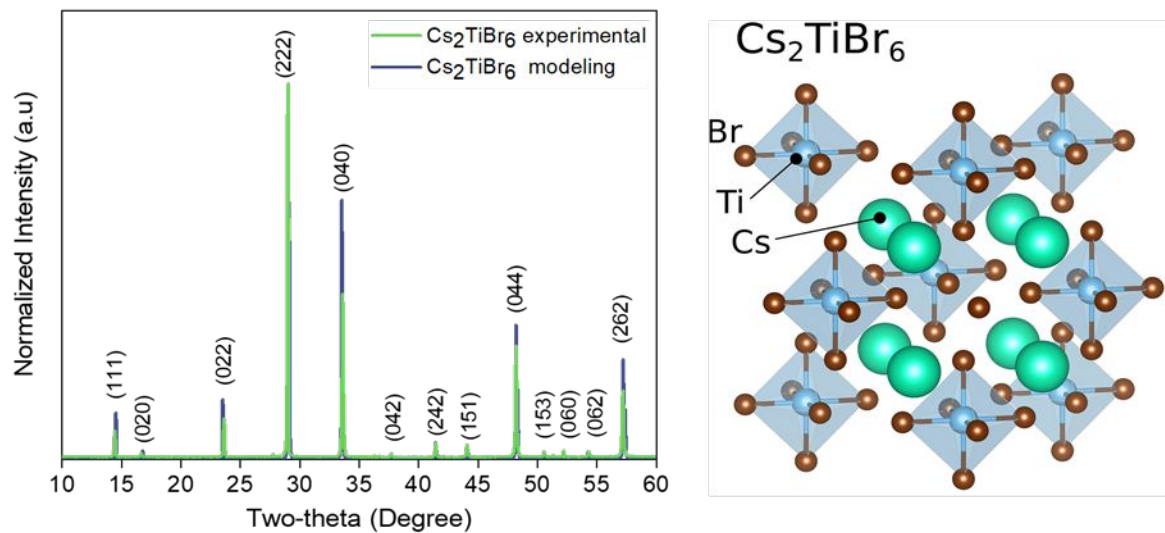


Figure S4. Comparison of XRD diffractograms for the optimized powders: experimental XRD pattern (in green) and simulated XRD pattern (in dark blue) developed *in silico* using DFT calculations and VASP code for the represented Cs₂TiBr₆ crystal structure.

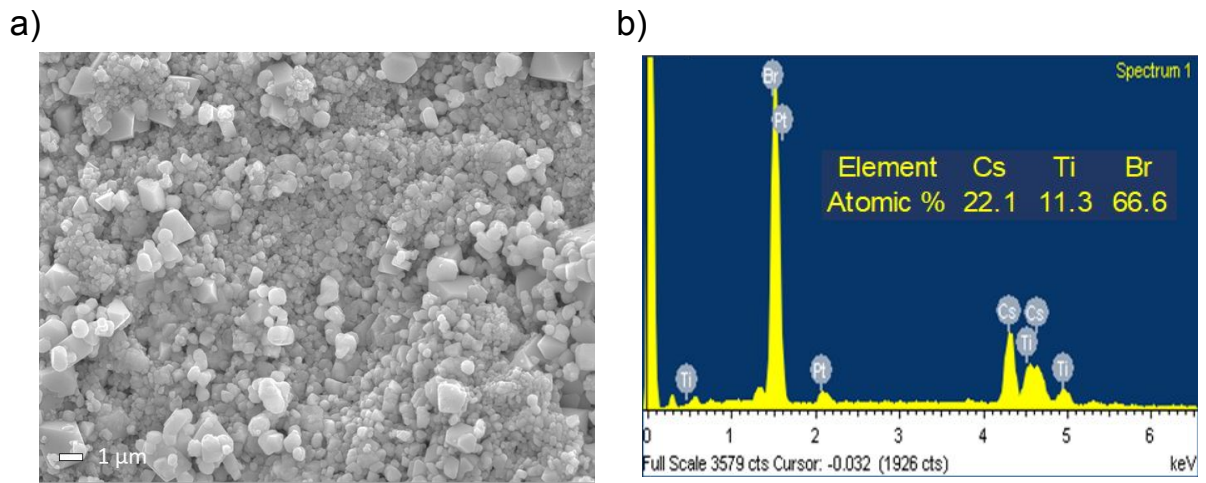


Figure S5. a) SEM photograph of Cs_2TiBr_6 powder, the scale bar represents 1 μm , b) EDS spectrum of the MW-synthesized Cs_2TiBr_6 powder including the Cs:Ti:Br atomic percentage, which fits well with Cs_2TiBr_6 element proportion.

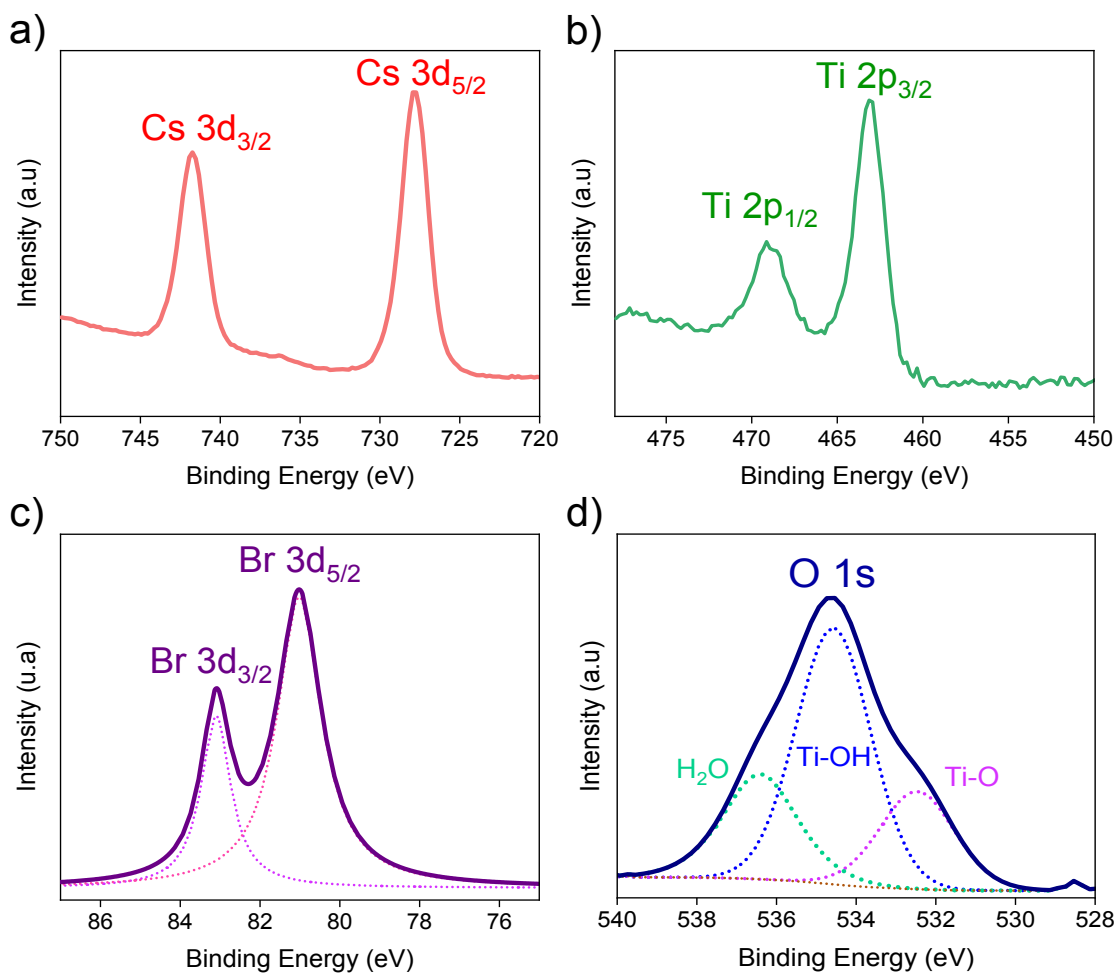


Figure S6. a) XPS spectra of the Cs_2TiBr_6 powder exhibit a high level of resolution for a) $\text{Cs } 3d$, b) $\text{Ti } 2p$, c) $\text{Br } 3d$, and d) $\text{O } 1s$ (including deconvolution of the different oxygen species present in the sample).